Phys. Status Solidi A **211,** No. 6, 1255–1258 (2014) / **DOI** 10.1002/pssa.201300130

physica status solidi a
www.pss-a.com
applications and materials science

Enhancement of the power factor in two-phase silicon–boron nanocrystalline alloys

Dario Narducci*[,1], Bruno Lorenzi[1], Xanthippe Zianni[2,3], Neophytos Neophytou[4,5], Stefano Frabboni[6,7], Gian Carlo Gazzadi[7], Alberto Roncaglia[8], and Francesco Suriano[8]

[1] Department of Materials Science, University of Milano Bicocca, Milan, Italy
[2] Department of Aircraft Technologies, Technological Educational Institution of Sterea Ellada, Psachna, Greece
[3] Department of Microelectronics, IAMPPNM, NCSR Demokritos, Athens, Greece
[4] Institute for Microelectronics, TUV, Vienna, Austria
[5] School of Engineering, University of Warwick, Coventry, UK
[6] Department of FIM, University of Modena and Reggio Emilia, Modena, Italy
[7] CNR–Institute of Nanoscience–S3, Modena, Italy
[8] IMM–CNR, Bologna, Italy

Received 17 May 2013, revised 23 December 2013, accepted 4 March 2014
Published online 15 April 2014

Keywords alloys, energy filtering, precipitates, silicon, thermoelectricity

* Corresponding author: e-mail dario.narducci@unimib.it, Phone: +39 02 64485137, Fax: +39 02 64485400

In previous publications it was shown that the precipitation of silicon boride around grain boundaries may lead to an increase of the power factor in nanocrystalline silicon. Such an effect was further explained by computational analyses showing that the formation of an interphase at the grain boundaries along with high boron densities can actually lead to a concurrent increase of the electrical conductivity σ and of the Seebeck coefficient S. In this communication we report recent evidence of the key elements ruling such an unexpected effect. Nanocrystalline silicon films deposited onto a variety of substrates were doped to nominal boron densities in excess of 10^{20} cm^{-3} and were annealed up to 1000 °C to promote boride precipitation. Thermoelectric properties were measured and compared with their microstructure. A concurrent increase of σ and S with the carrier density was found only upon formation of an interphase. Its dependency on the film microstructure and on the deposition and processing conditions will be discussed.

1 Introduction The rush for high-efficiency thermoelectric materials has undergone a sudden acceleration over the last decade. On one side, efficiency could be improved in dimensionally limited systems such as nanowires, that display lowered thermal conductivities κ while preserving their electrical conductivities σ and their Seebeck coefficients S [1–3]. On the other side, enhancements of the power factor $P\ S^2\sigma$ was shown to occur in some systems by straining [4], energy filtering [5], δ-doping [6, 7] and quantum confinement [8]. All approaches lead to increased figures of merit $Z\ P/\kappa$, although material usability in practical contexts may quite differ whether high Z-values are due to low thermal conductivities or to high power factors [9].

In previous publications [10–12], we reported that annealing polycrystalline silicon doped with boron by ion implantation at total final densities in excess to boron solid solubility leads to an unexpected simultaneous increase of both the electrical conductivity and of the Seebeck coefficient. Such a finding, strikingly counterintuitive for diffusive charge transport, was shown [13, 14] to be possible in a composite, two-phase system if (a) carriers are energy filtered at potential barriers, (b) charge transport involves high energy carriers and (c) the phase showing the largest Seebeck coefficient is also characterised by the lowest thermal conductivity. Thus, provided that processing of heavily doped silicon leads to the formation of a silicon–silicon boride two-phase system, where silicon boride precipitates have sizes of a few nanometers and silicon grain size is comparable to the majority carrier energy-relaxation mean free path.

This paper reports the first experimental validation of the model presented in Refs. [13, 14]. A variety of silicon-based systems meeting only some of the model requirements were prepared, changing dopant concentration and material micromorphology (i.e. grain size and orientation). Micromorphology was modified by changing the substrate and the deposition conditions. Substrates were chosen so that their different thermal resistances might promote the growth of films with different grain sizes and shapes. This allowed to verify whether the anomalous increase of the power factor actually requests all the ingredients the model predicts as needed. It will be shown that the anomalous growth of the power factor at the highest annealing temperatures T_a actually requires the concurrent presence of a nanograined morphology along with the formation of boron-enriched nanoprecipitates.

2 Experimental Table 1 summarises the characteristics of all samples studied in this paper. In short, three types of substrates were used, namely oxidised silicon (S family), a SiO_x–Si_3N_4 bilayer deposited onto oxidised silicon (T family) and a silica substrate (Q sample). Polycrystalline films were all deposited by chemical vapour deposition (CVD). Silane was used, always keeping the substrate at 610 °C but for sample S1, for which a deposition temperature of 600 °C was chosen. In addition, silicon-on-insulator (SOI) single crystalline films were also analysed. All samples were boron doped by ion implantation at different doses and energies to obtain degenerate silicon films with nominal boron densities ranging around its solubility threshold at 500 °C [15]. After damage recovery, samples underwent sequential thermal treatments up to 1000 °C in argon, each step lasting 2 h. Al–Si 5% pads were evaporated for all transport measurements and were removed by HCl followed by piranha etch (H_2O_2 33 vol% + H_2SO_4 98 vol% in a 1:2 ratio, 95 °C, 30 min) prior to the subsequent annealing.

Electrical conductivity, Hall effect, and Seebeck coefficient measurements were carried out. Conductivity was determined by current–voltage characteristics at 20 °C. Measurements of σ as a function of the temperature confirmed for all samples a negative temperature coefficient as expected in a degenerate semiconductor. Samples for the Seebeck and the electrical conductivity measurements were obtained by cutting $50 \times 5\,mm^2$ rectangular chips and evaporating metal contacts through a shadow mask. For Hall measurements, $17 \times 17\,mm^2$ samples were cut and metal contacts were evaporated on small areas in the four corners according to the Van der Pauw geometry. Hall measurements were carried out at room temperature with a maximum magnetic field of 0.5 T. Seebeck coefficient was measured using a lab-made apparatus that was calibrated toward single-crystal silicon samples of known doping level. The apparatus allowed for temperature differences up to 80 °C. Each set of measurements was repeated on the same sample at least three times to ensure data reliability. Further details concerning the experimental setup are reported elsewhere [10].

Cross-sections for electron microscopy (EM) analyses were prepared by conventional methods, grinding, polishing and finally thinning the samples with an argon ion beam. EM analyses were performed both in low-energy (30 keV) dark field scanning transmission (DF-STEM) and in high-energy (200 keV) transmission (TEM) modes. Low-energy analyses were performed with a FEI Strata235M equipped with bright field–dark field solid state detector. TEM and energy filtered electron spectroscopic images (ESI) were obtained using a JEM2011 electron microscope (spherical aberration coefficient 0.5 mm, chromatic aberration coefficient 1.1 mm) equipped with conventional LaB_6 electron source and an electron energy loss imaging filter (GIF 200®). This attachment allows to record both electron energy loss spectroscopy data and ESI.

3 Results As mentioned, annealing of sample S1 led to an unexpected increase of the power factor as a result of the concurrent increase of its electrical conductivity and of the Seebeck coefficient. Hall effect measurements showed that annealing at temperatures higher than 800 °C resulted in a decrease of the majority carrier density p due to the precipitation of metastable substitutional boron. This causes the formation of potential barriers and obviously leads to an increase of S. The unexpected finding was that also the hole drift mobility μ_D steeply increased, overcompensating the detrimental effect of the lower carrier density on σ. Figure 1 summarises the experimental dependency of both μ_D and S

Table 1 Summary of the samples analysed in this paper. Families S, T and Q refer respectively to thin films deposited onto oxidised silicon, a Si_3N_4 layer deposited onto oxidised silicon, and vitreous silica. Symbols ∥ and ⊥ label directions referred to the substrate.

ID	thickness (nm)	ion implantation energy (keV)	dose (cm^{-2})	total boron density (cm^{-3})	damage recovery conditions	grain size (nm)	second phase
S1	450	60	2.0×10^{16}	4.4×10^{20}	1050 °C, 30 s	100⊥, 30–50∥	observed
S2	200	30	0.4×10^{16}	2.0×10^{20}	1100 °C, 300 s	100⊥, 30–50∥	absent
S3	200	30	0.8×10^{16}	4.0×10^{20}	1100 °C, 300 s	100⊥, 30–50∥	absent
S4	200	30	1.2×10^{16}	6.0×10^{20}	1100 °C, 300 s	80–100⊥, 50–100∥	observed
T1	200	30	1.2×10^{16}	6.0×10^{20}	1100 °C, 300 s	80⊥, 50–100∥	absent
T2	200	30	0.4×10^{16}	2.0×10^{20}	1100 °C, 300 s		
Q1	490	40	2.5×10^{16}	5.1×10^{20}	1100 °C, 300 s	100⊥, 100–150∥	observed
SOI	342	50	2.5×10^{16}	3.5×10^{20}	1100 °C, 300 s	–	

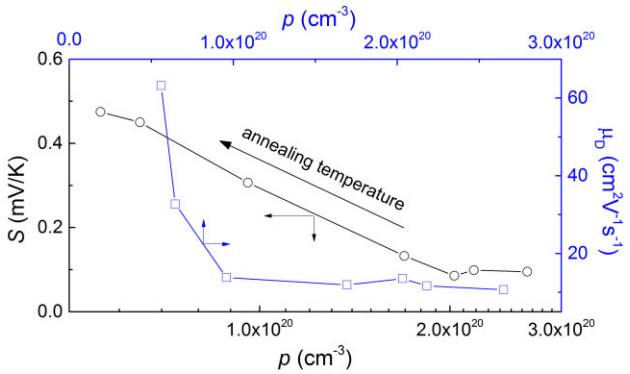

Figure 1 Experimental dependency of drift mobility and Seebeck coefficient on the hole density for sample S1. Carrier density was modulated by sequential annealing at increasing temperatures that promotes a gradual precipitation of boron.

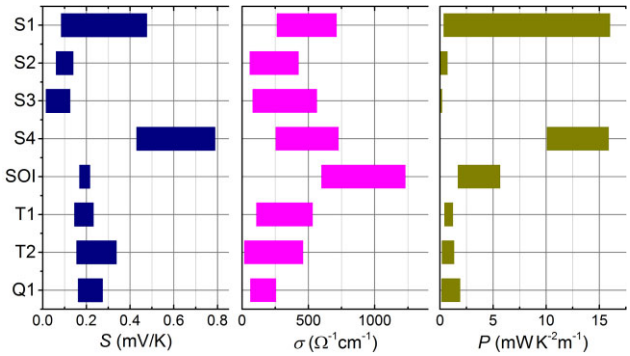

Figure 3 Variation of the thermoelectric coefficient, the electrical conductivity and the power factor as a result of thermal processing up to 1000 °C on samples described in Table 1.

on p. TEM analyses (Fig. 2) showed that, while the thermal processing did not significantly modify the grain size, it caused a precipitation of a boron-rich second phase around the grain boundaries – not decorating the grain boundaries themselves. Such a unique feature is known and reported in literature for boron [16], and encouraged to correlate the anomalous dependency of the mobility to the formation of potential barriers associated to the presence of precipitates. All polycrystalline films exhibited columnar growth, with grain aspect ratio somewhat larger in the S than in the T or Q families.

Figure 3 reports a comparison of the span of S, σ, and of the power factor measured on the samples considered in this work and consequent to the thermal processing.

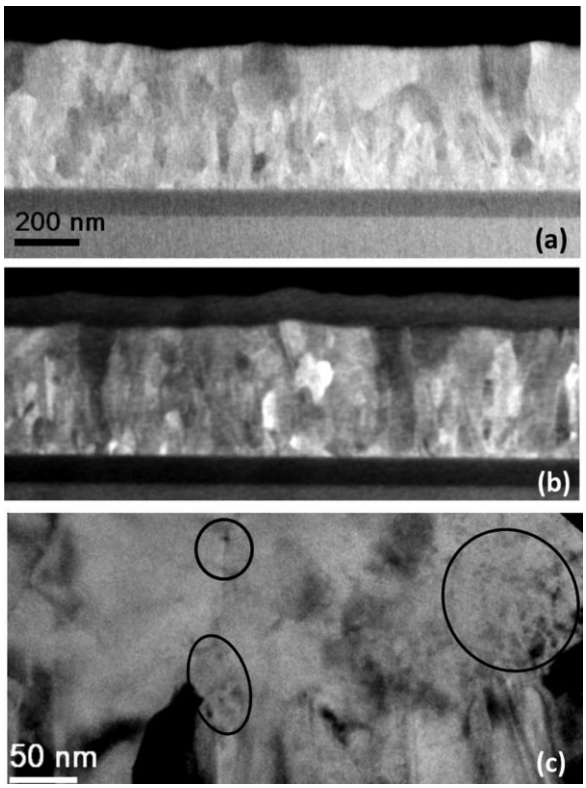

Figure 2 (a) DF-STEM image of the as-deposited S1 sample; (b) DF-STEM and (c) TEM bright field image of the same sample, both taken after annealing at 1000 °C. Circled areas in the TEM image mark diffraction contrast details due to the precipitation of a second phase. Note the preservation of grain sizes upon annealing at high temperature.

4 Discussion Of the three features considered as possibly responsible for the increase of the power factor, the role of degeneracy in itself can be immediately discarded. Single-crystalline SOI film, although degenerate, did not display any increment of the power factor significantly above the value theoretically expected for silicon ($\approx 3\,\mathrm{mW\,K^{-2}\,m^{-1}}$ [17]). This is in good agreement with a rather large body of previous studies on heavily doped silicon [17–19]. Not even the precipitation of a second phase, expected for a heat-treated material with a nominal boron density $> 2 \times 10^{20}\,\mathrm{cm^{-3}}$ appears to be sufficient to determine the mobility enhancement observed in S1.

Moving to polycrystalline films, the role played by the total boron concentration is quite evident comparing samples from the S and T families. Whenever boron content is lower than $4 \times 10^{20}\,\mathrm{cm^{-3}}$, no precipitation of boron is either expected or observed – and no anomalous increase either of the mobility or of the power factor is found. It may be worthwhile to stress that the actual formation of boron precipitates is not simply related to thermodynamic considerations. Apart from the effect on the solubility threshold of grain boundaries and their eventual decoration [20], the formation of a second phase upon relatively short (2 h) heat treatments is also ruled by boron diffusivity. Using standard models [21] it can be verified [22] that, in the range of temperature–time conditions considered in this study, boride precipitation occurs only for initial boron concentrations exceeding $\approx 4 \times 10^{20}\,\mathrm{cm^{-3}}$. This is consistent with our experimental results, where no formation of boron-rich second phase was actually observed for lower initial boron densities.

Boron supersaturation is not however sufficient to induce a power factor enhancement. While actually sample S4 reports a power factor value comparable to that observed on S1, no likely effect is observed either on sample T1 or Q1. Interestingly enough, sample Q1 displays a concurrent increase of S and σ upon annealing, but the final power factor value it reaches after the heat treatment at 1000 °C is about one order of magnitude lower than that observed in S1. A key to understand such a difference is in the grain size, much larger for Q1 than for S1. Since, according to the model, energy filtering is proportional to the volume of grain boundaries and its effect is larger when energy relaxation within the grains is less efficient (i.e. when grain size is small), it is not unreasonable to conclude that carrier filtering is active but less effective in Q1, explaining its lower performances.

Sample T1 is more puzzling. Absence of a second phase clearly explain the lack of power factor enhancement. Yet it is not immediate to understand why, in spite of the high nominal boron density, no precipitation occurs upon annealing. In principle, since diffusivity in polycrystalline materials strongly depends on the structure of grain boundaries, a larger abundance of grains oriented along [311] (reported by TEM) might provide a rationale to the observed metastability of the boron–silicon solution. Nonetheless, further investigations are surely needed to obtain a fully convincing explanation for the absence of precipitates.

5 Summary and conclusions To the best of our knowledge, this paper is the first systematic investigation pointing out an enhancement of the power factor in p-type heavily doped polycrystalline silicon due to carrier energy filtering. Based upon the comparison of eight samples differing by micromorphology and boron concentration it seems sensible to conclude that an enhancement of the power factor in silicon does require the concurrency of (a) a grain size enabling only partially energy-relaxed carrier transport, high boron doping enabling high velocity carriers to participate in transport; and (b) the presence of suitable energy filtering barriers preventing slow carriers from participating in the energy and charge transport. Grain sizes from 30 to 50 nm (cf. samples S1 and S4) were found to best suit such requirements. These results apparently corroborate the transport model previously proposed. Energy filtering in single crystals and in relatively large-grained polycrystalline materials only partially compensates the reduction of σ resulting from a decrease of the actual carrier density. No simultaneous increase of the thermopower and of the electrical conductivity is found as charge transport occurs in the diffusion regime, so that carrier relaxation dumps the effect of energy filtering on μ_D. Instead, in nanocrystalline systems with grains small enough to allow only partial carrier energy relaxation, filtering fully enables the participation of fast carriers only to conduction, leading to the observed overcompensation of the lowered carrier density.

Acknowledgement Preparation of Q1 sample by Dr. Georg Pucker (Fondazione Bruno Kessler, Italy) is gratefully acknowledged.

References

[1] A. I. Hochbaum, R. K. Chen, R. D. Delgado, W. J. Liang, E. C. Garnett, M. Najarian, A. Majumdar, and P.D. Yang, Nature **451**(7175), 163–1167 (2008).
[2] A. I. Boukai, Y. Bunimovich, J. Tahir-Kheli, J. K. Yu, W. A. Goddard, and J.R. Heath, Nature **451**(7175), 168–1171 (2008).
[3] M.G. Kanatzidis, Chem. Mater. **22**(3), 648–659 (2009).
[4] N. F. Hinsche, I. Mertig, and P. Zahn, J. Phys.: Condens. Matter **24**(27), 275501 (2012).
[5] A. Popescu, L. M. Woods, J. Martin, and G.S. Nolas, Phys. Rev. B **79** (May), 205302, (2009).
[6] T. Koga, S. Cronin, M. Dresselhaus, J. Liu, and K. Wang, Appl. Phys. Lett. **77**(10), 1490–1492 (2000).
[7] B. Yu, M. Zebarjadi, H. Wang, K. Lukas, H. Wang, D. Wang, C. Opeil, M. Dresselhaus, G. Chen, and Z. Ren, Nano Lett. **12**(4), 2077–2082 (2012).
[8] A. Bulusu, D.G. Walker, Superlattices Microstruct. **44**(1), 1–36 (2008).
[9] D. Narducci, Appl. Phys. Lett. **99**(10), 102104 (2011).
[10] D. Narducci, E. Selezneva, A. Arcari, G. Cerofolini, E. Romano, R. Tonini, and G. Ottaviani, in: MRS Online Proc. Library, Vol. 1314 (MRS, 2011), mrsf10-1314-ll05-16.
[11] D. Narducci, E. Selezneva, G. Cerofolini, S. Frabboni, and G. Ottaviani, AIP Conf. Proc. **1449**(1), 311–314 (2012).
[12] D. Narducci, E. Selezneva, G. Cerofolini, S. Frabboni, and G. Ottaviani, J. Solid State Chem. **193**, 19–25 (2012).
[13] N. Neophytou, X. Zianni, M. Ferri, A. Roncaglia, G. Cerofolini, and D. Narducci, J. Electron. Mater. **42**(7), 2393–2401 (2013).
[14] N. Neophytou, X. Zianni, H. Kosina, S. Frabboni, B. Lorenzi, and D. Narducci, Nanotechnology **24**(20), 205402 2013.
[15] G. L. Vick and K. M. Whittle, J. Electrochem. Soc. **116**(8), 1142–1144 (1969).
[16] M. M. Mandurah, K. C. Saraswat, C. R. Helms, and T. I. Kamins, J. Appl. Phys. **51**(11), 5755–5763 (1980).
[17] T. H. Geballe and G. W. Hull, Phys. Rev. **98**(4), 940 (1955).
[18] W. Fulkerson, J. P. Moore, R. K. Williams, R. S. Graves, and D. L. McElroy, Phys. Rev. **167**(3), 765 (1968).
[19] C. N. Liao, C. Chen, and K. N. Tu, J. Appl. Phys. **86**(6), 3204–3208 (1999).
[20] X. Luo, S. B. Zhang, and S. H. Wei, Phys. Rev. Lett. **90**(2), 026103 (2003).
[21] F. S. Ham, J. Phys. Chem. Solids **6**(4), 335–351 (1958).
[22] D. Narducci, E. Selezneva, G. Cerofolini, E. Romano, R. Tonini, and G. Ottaviani, in: Proc. 8th European Thermoelectric Conf., (CNR, Como, 2010), pp. 141–146.

